Environmental Science and Pollution Research (2019) 26:7810–7820
https://doi.org/10.1007/s11356-019-04147-9

RESEARCH ARTICLE

# Sono-advanced Fenton-like degradation of aromatic amines in textile dyeing sludge: efficiency and mechanisms

Haiyuan Zou[1] · Xun-an Ning[1] · Yi Wang[1] · Jian Sun[1] · Yanxiang Hong[1]

Received: 15 November 2018 / Accepted: 2 January 2019 / Published online: 24 January 2019


## Abstract

In this paper, a novel strategy integrating ultrasound (US) with a Fenton-like (zero-valent iron/EDTA/air, ZEA) process was proposed for the removal of the refractory and carcinogenic aromatic amines (AAs) in textile dyeing sludge for the first time. The operating condition was optimized as 1.08 W/cm$^3$ ultrasonic density, 15 g/L ZVI, and 1.0 mM EDTA, which could reach degradation efficiencies of 51.79% in US, 72.88% in ZEA, and 92.40% in US/ZEA system after 90-min reaction. Quenching experiments showed that electron transfer reactions generated by the iron ligands in ZEA brought about various reactive oxidative species (ROS), in which Fe (IV), $O_2^{\cdot-}$, and $^{\cdot}OH$ dominated the degradation. US induced sludge disintegration by ultrasonic shear, proven by particle size decrease and supernatant organic matter upsurge, which helps ROS contact with those pollutants in the sludge cavities. Besides, US facilitated the iron redox cycle for oxygen activation by promoting the corrosion of ZVI and stripping considerable ferric ions from sludge iron oxides which were verified by SEM, XRF, and XPS.

**Keywords** Ultrasound · Textile dyeing sludge · Aromatic amines · Fenton-like process · Persistent organic pollutants · Environmental remediation

## Introduction

Textile dyeing sludge (TDS) is a non-negligible threat to human health and the environment due to its tremendous yield and complexity (Meng et al. 2016), making it difficult to be safely treated and disposed of (landfill and incineration). Thus, it has been classified as a strict control waste (HY02) in Guangdong Province, China.

Among those POPs determined in TDS, aromatic amines (AAs), which are often used as the components of azo dyes, are distinguished due to their highly teratogenic, carcinogenic, and mutagenic properties (Ning et al. 2015). To date, AAs have been banned by the European Union (Regulation 1907/2006) as well as China (GB/T 17592-2011), but the decomposition of dyes with complicated structure still brings about the detection of these compounds during the wastewater treatment (Ning et al. 2015). After wastewater treatments, these residues would be in large quantity aggregating and adsorbing onto the surface and the cavities of sludge (Lin et al. 2016). During the sludge's landfill process, soil amendment, or compost, the bioavailable portion of these contaminants would be concentrated in plants and organisms (Stefaniuk et al. 2018), exhibiting strong phytotoxicity or cytotoxic and genotoxic effects (Sommaggio et al. 2018). Thus, additional post-treatments for efficacious removal of these contaminants are in urgent demand (Deng et al. 2018).

Advanced oxidation processes (AOPs) have long been considered as effective technologies for the removal of recalcitrant organic pollutants, such as PAHs (Lin et al.

**Highlights**
- Application of US and ZEA to textile dyeing sludge removes a large amount of AAs.
- The promotional role of US in ZEA system is clarified.
- Pristine iron in sludge participates in the iron redox cycle of the ZEA process.
- Iron oxides in sludge can induce a heterogeneous ZEA reaction.

Responsible editor: Vítor Pais Vilar

**Electronic supplementary material** The online version of this article (https://doi.org/10.1007/s11356-019-04147-9) contains supplementary material, which is available to authorized users.

✉ Xun-an Ning
ningxunan666@126.com; 1427013409@qq.com

[1] School of Environmental Science and Engineering, Institute of Environmental Health and Pollution Control, Guangdong University of Technology, Guangzhou 510006, China

2016) and PPCPs (Huang et al. 2017). Among AOPs, those based on zero-valent iron (ZVI) have been widely used due to their cost-effective, highly efficient, and environment-friendly properties (Segura et al. 2015; Tao et al. 2016). In a ZVI/air system, the mechanism for oxygen activation mainly involves two proportions (Lee et al. 2014), including the production of $H_2O_2$ in situ and the subsequent Fenton reactions generating reactive oxidative species (ROS), which are competent in oxidizing organic pollutants non-selectively. However, the ROS yield is considerably low. In addition, surface passivation, i.e., the formation of an iron oxide/hydroxide layer triggered by the corrosion of ZVI at circumneutral conditions, also limits ZVI application (Ghods et al. 2011). To vanquish these issues, the addition of iron-chelating ligand like EDTA (Englehardt et al. 2007) has proved efficacious in coordinating with the surface-bound ferrous ions to block the formation of iron (hydro)oxide layer. Meanwhile, EDTA's coordination products would complex dissolved oxygen and produce $H_2O_2$; thus, the production of ROS would be boosted.

Nevertheless, the oxidation performance of ZVI/EDTA/air (ZEA) process is generally retarded by the slow heterogeneous interfacial reactions (Li et al. 2014). Therefore, the introduction of ultrasound (US) was proposed. As reported by Sivasankar and Moholkar (2009), US can expectedly break down the passive film on the ZVI surface and boost the mass transfer via its cavitation effect. Besides, ultrasonic shear (Bagal and Gogate 2012, 2014) can also homogenize the ROS connection with contaminants absorbed onto the surface or the cavities of the solid matrix. Previous research has shown that the combination of US and advanced Fenton process has great potential for the removal of recalcitrant imidacloprid (Patil et al. 2014), as well as the treatment of landfill leachate (Joshi and Gogate 2019). In addition, this combined process is not restricted to wastewater treatment. The application of ultrasound combined with advanced Fenton process has also been used to treat oily sludge (Zhang et al. 2013) and textile dyeing sludge (Lin et al. 2016), and high removal efficiencies of hydrocarbons were obtained. However, to our knowledge, study done on US combining ZEA for the removal of recalcitrant AAs in textile dyeing sludge has not yet been reported.

Therefore, the scope of the present study comprised of the following: (1) investigation of several significant experimental parameters on AA degradation in different systems; (2) verification of the enhanced degradation of AAs in the ZEA system integrated with US; (3) exploration of the role of sludge iron functions in the EDTA/air system; (4) identification of the dominant ROS in the US/ZEA system; and, (5) revelation of the stimulative role of ultrasound therein.

## Materials and methods

### Materials

Mixed aromatic amines (300 mg/L in methanol) were obtained from O2si Smart Solutions (Charleston, SC, USA) with a purity > 99.5%, including 2,4,5-trimethylaniline (TMA), 2-naphthylamine (NA), 4-4-aminoazobenzene (AAB), O-aminoazotoluene (o-AOT), and 3,3′-dichlorobenzidine (DB). ZVI particles (purity > 99%, below 400 mesh) and other common chemicals of analytical grade, such as NaOH, HCl, dimethyl sulfoxide (DMSO), and tert-butyl alcohol (TBA), were obtained from Aladdin (Shanghai, China). Ethylenediaminetetraacetic acid disodium dihydrate salt (purity 99.0–101.0%) as well as organic solvents of high-performance liquid chromatography (HPLC) grade were purchased from CNW Technologies GmbH (Düsseldorf, Germany). Superoxide dismutase (SOD, 98% protein, 3000 U/mg protein) and catalase (CAT, 2000–5000 U/mg protein) were from Sigma-Aldrich (St. Louis, USA). Preparation of all solutions was done using deionized water with resistivity of 18.25 MΩ cm.

Textile dyeing sludge samples were collected from a textile wastewater treatment plant in Guangzhou (Guangdong Province, China). Considering the inconvenience of high-moisture-content sludge with respect to storage and transportation, sludge after dehydration using a belt filter press was collected from the final storage container. The samples were, then, stored in a freezer at 4 °C prior to reaction and analysis. The details of the treatment procedure, materials, and dyes used in the textile dyeing plants, and the characteristics of the textile dyeing sludge are given in Table 1.

### Experimental procedure

The experiments on the degradation of AAs in textile dyeing sludge were conducted in a 0–1800 W sonicator (Scientz JY99-IIDN, China, 20 kHz) equipped with a sealed converter and a titanium probe tip (25 mm in diameter and 320 mm in length). The energy transfer efficiency of the sonicator was calculated by calorimetric method following the mathematical Eq. (2) (Mhetre and Gogate 2014). Noticeably, the calorimetric efficiency was almost constant at 56% (Table S2). The specific calculation procedure was shown in Supplementary Information (Test S1). The temperature was maintained at 25 ± 1 °C using a cylindrical reactor with a circulating temperature controller. The experimental set-up and the actual apparatus are shown in Fig. S1. Driven by an air pump, air (1.0 L/min) was evenly and continuously supplied to the slurry through a porous aerator fixed at the bottom of the reactor. A mechanical mixer (200 rpm) was used to promote uniform mixing in the water–sludge system during the Fenton-like process, but the ultrasonic power could also well mix the

**Table 1** Characteristics of the raw textile dyeing sludge

| Main treatment processes | Dyes | Textile material | pH | Moisture content (%) | Organic content (%) | AAs (mg/kg) | | | | |
|---|---|---|---|---|---|---|---|---|---|---|
| | | | | | | TMA | NA | AAB | o-AAT | DB |
| Flocculation, A/O | Reactive | Cotton | 8.70 | 63.60 | 34.56 | 1.28 | 5.00 | 16.19 | 10.71 | 5.14 |

water–sludge mixture without the stirrer during the ultrasound and US/ZEA process.

$$Q = m \cdot C_P \cdot \triangle T \quad (1)$$

$$\eta = \frac{\text{Amount of energy gained by sludge}}{\text{Electrical energy input}} \times 100\% = \frac{m \cdot C_p \cdot \triangle T}{Et} \times 100\% \quad (2)$$

where $m$ is mass of the medium (kg), $C_p$ is specific heat capacity in kJ/(kg·°C), $\triangle T$ is temperature change (°C), $E$ is electric energy input (W), and $t$ is time required for temperature to increase by 1° (s).

According to the moisture content of the sludge produced in real conditioning unit, the sludge samples (500 mL, 98% moisture content) were prepared by blending dewatered sludge with corresponding amount of ultrapure water before oxidation. After addition of EDTA into the sludge samples, ZEA reaction was then initiated by adding ZVI, and ultrasonic radiation was exposed at the same time. The quenching experiments were initiated with the addition of SOD (1500 U/L), CAT (150 mg/L), TBA (100 mM), and DMSO (100 mM). After the treatment, the periodically withdrawn slurry was centrifuged at 4000 rpm for 10 min and the solid residue was, then, freeze-dried (− 60 °C, 12 h), manually crushed, and sieved (by 200 mesh) prior to chemical analysis. The supernatant was quickly filtered through a 0.22-mm membrane for further analyses.

## Analytical methods

Quantification of AAs was done by Agilent 7890B gas chromatograph-5977B mass spectrometer (GC-MS, Agilent, USA). Chromatographic separation was carried out by a HP-5MS column (30 m × 0.25 mm, film thickness of 0.25 m, Agilent, USA). The presentation of further details about the extraction of AAs and GC/MS analytical conditions are shown in the Supplementary Information (Text S1). Analyses with procedural blanks, spiked blanks, and sample duplicates or triplicates were routinely performed for every batch of samples.

The pH was adjusted with 0.1 M sulfuric acid ($H_2SO_4$) and/or 0.1 M sodium hydroxide (NaOH) if necessary and detected using a pH meter (pHS-3C, Leici, China) at room temperature. Sludge organic matter (SOM) content was measured by loss-on-ignition (Lin et al. 2016). Dissolved organic carbon (DOC) of the supernatant was directly detected by a TOC-L CPH analyzer (Shimadzu, Japan). 1,10-Phenanthroline was used for the determination of $Fe^{2+}$ and total dissolved iron (TFe) by UV–Vis spectrophotometer (Cary 100, Agilent, USA) at a wavelength of 510 nm (Jr et al. 1955). More details of these analyses are revealed in the Supplementary Information (Text S2).

## Sludge and ZVI characterization

The metal oxide composition of sludge was detected by an energy-dispersive X-ray fluorescence spectrometer (EDX-7000, Shimadzu, Japan). XPS was conducted using an X-ray photoelectron spectroscopy spectrometer (Thermo Scientific ESCALAB 250Xi), with a monochromatized Al X-ray source, which was operated at a power of 150 W. Particle size of the sludge before and after treatment was also measured by a Laser Particle Size Analyzer (Mastersizer 3000E, Malvern, UK).

After different reactions for 60 min, the precipitated ZVI were thoroughly rinsed by $N_2$-sparged ultrapure water until there was no sludge particle mixing; then, ethanol with gradient concentrations was used for secondary cleanout; and, finally, the samples were freeze-dried for 12 h to avoid the changing of the ZVI surface oxidation layers. Coated with an electrically conductive Au surface layer, the morphology of these ZVI specimens was obtained by the cold field-emission scanning electron microscope (FESEM, SU8010, Hitachi).

# Results and discussion

## Effects of experimental parameters on AA degradation

Based on our previous preliminary experiments, several operational parameters, namely, ultrasonic density, ZVI loading, EDTA dosage, and initial pH were analyzed on the degradation of AAs in different systems, with corresponding extents of 0.36–2.16 W/cm$^3$, 5–30 g/L, 0–3.0 mM, and 3–11. The obtained consequences were illustrated in Fig. 1.

### US density

The removal efficacies of AAs under different ultrasonic densities (0.36, 0.72, 1.08, 1.44, 1.80, 2.16 W/cm$^3$) in the US system are shown in Fig. 1a. As illustrated, a gradual decay was seen in each aromatic amine as the ultrasound density

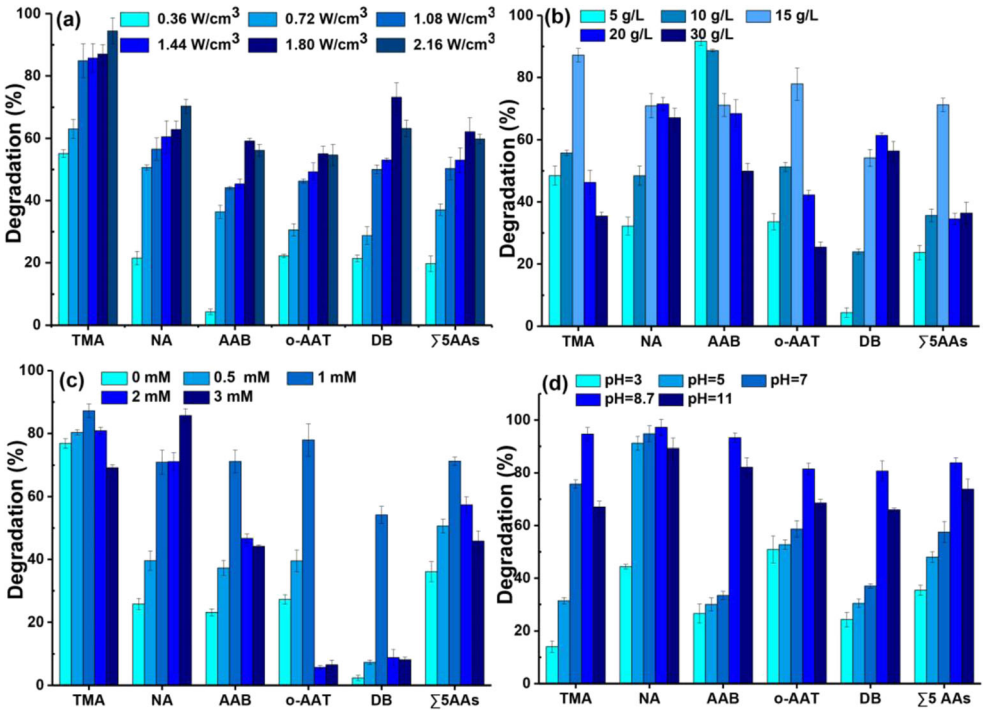


**Fig. 1** Effects of initial (**a**) ultrasonic power, (**b**) ZVI dosage, (**c**) EDTA dosage, and (**d**) pH on the degradation of AAs in US (**a**), ZEA (**b**, **c**), and US–ZEA (**d**) system. The initial experimental conditions were 1.08 W/cm$^3$ sonic density, 15 g/L ZVI, 1 mM EDTA, and ambient pH and temperature, except for the investigated parameters

grew, reaching to the maximum of 62.1% total removal with 1.80 W/cm$^3$ ultrasound density. Accountably, the generation of ˙OH increased with the strengthening of the ultrasonic density, leading to a more intensive oxidizing effect of AAs. However, sonication with higher density (2.16 W/cm$^3$) showed lower efficiencies on the degradation of AAB, o-AAT, and DB. This was consistent with previous studies on the degradation of aromatic hydrocarbon by ultrasound (Lin et al. 2016). Organic pollutants with higher molecular weight have higher oxidation potential (Lee et al. 2001), and, therefore, would be degraded preferentially than these low-molecular-weight aromatic amines. The monocyclic aniline, however, was much easier to break down by ultrasonic oxidation, thus reaching to a degradation efficiency of 94.44%. Although an optimal ultrasonic density (1.80 W/cm$^3$) was obtained, it was too high to have benefits for subsequent sludge dewaterability (Li et al. 2009). Considering energy consumption and the efficiency of subsequent TDS dewatering, 1.08 W/cm$^3$ was chosen as the optimal sonic density for AA degradation in TDS during the ultrasound process.

## Iron loading

In the ZEA system, zero-valent iron functions an indispensable role in generating ferrous ions by its oxidation and reducing ferric ions to the ferrous ones so as to prompt the iron circulation, which was verified by the relatively constant amounts of $Fe^{2+}$ (5.0–8.5 mg/L) and $Fe^{3+}$ (11.7–14.7 mg/L), shown in Fig. 2a. It was reported (Cai et al. 2016) that ZVI would lead to both the formation of soluble $Fe^{2+}$ and the generation of $\{Fe{\cdot}Fe^{2+}\}$ adsorbing on the ZVI surface and that instead of the generated homogeneous Fenton reaction, it was the heterogeneous catalytic reaction on the ZVI surface modified by EDTA that dominated the degradation (Zhou et al. 2014). This could explain the decrease of the aqueous-phase $Fe^{2+}$ concentration in the US/ZEA (Fig. 2a), for more surface-localized $Fe^{2+}$ was favorable for the enhancement of the degradation effect.

Figure 1b shows the effects of ZVI dosage on AA removal in the ZEA system. As presented, the degradation rates of four AAs could be accelerated as the iron loading increased to 15 g/L, but it would be retarded as the dosage further ascended to 30 g/L, with $\sum_5$AA removal efficiency decreased by 35.2%. The moderate increase of ZVI could promote the generation of $Fe^{II}$EDTA and $Fe^{III}$EDTA and the mutual transformation from one to another, thus propelling the activation of molecular oxygen. However, a report showed that overdose of ZVI would consume quite a number of $H_2O_2$ or react with oxygen species produced in site (Huang and Zhang 2005), which would overwhelm the abovementioned advantages. However, AAB shows a different trend compared with other four AAs, with a stably continuous decrease following the rise of ZVI addition. This could be addressed by the greater competitive edge of AAB toward other AAs as well as EDTA on the consumption of limited ROS.

## EDTA dosages

EDTA plays a significant role in ZEA reaction due to its enhancing effects in ZVI corrosion and the activation of

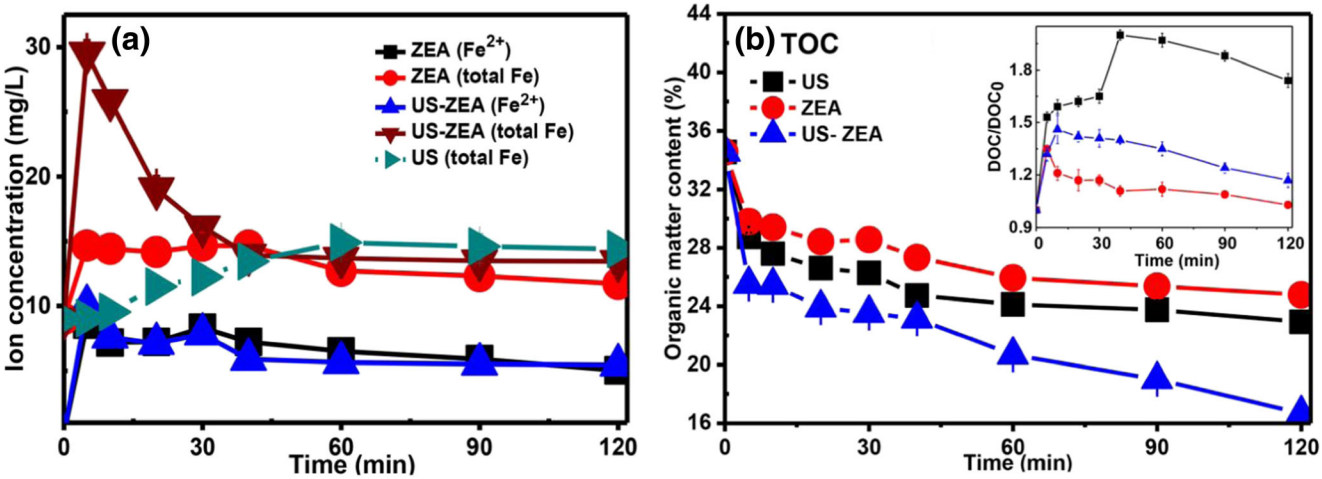


**Fig. 2** (**a**) Dissolved $Fe^{2+}$ and total Fe and (**b**) changes of SOM (the inset shows the TOC in the filtrate) in multiple systems. Initial condition: ZVI = 15 g/L; EDTA = 1.0 mM; ultrasonic power = 1.08 W/$cm^3$ under natural conditions

molecule oxygen over the ZVI surface in situ (Zhou et al. 2010); thus, investigation was carried out with various dosages of EDTA (i.e., 0, 0.5, 1.0, 2.0, and 3.0 mM). As revealed in Fig. 1c, EDTA addition showed an alike trend as the cases of iron loading (the "Iron loading" section), but the impact was more paramount, in which merely 5.72% of o-AAT and 8.83% of DB were degraded when the dosage increased to 2 mM. Thus, it can be concluded that EDTA presented forceful inhibition against other contaminants in the ZEA system, which was supported by And and Cheng (2005) that EDTA itself would deplete ROS generated especially when the amount was excessive. Therefore, the ratio of ZVI/EDTA should strike a balance to achieve significant degradation of AAs.

### Initial pH

Figure 1d delineates the degradation of selected AAs treated for 60 min at different initial pH values (i.e., 3.0, 5.0, 7.0, 8.6, 11). Interestingly, in this study, satisfactory removal efficiency was unavailable at acidic circumstances in the US/ZEA system, with merely 35.4 and 48.0% of AAs removed at pH 3.0 and 5.0, respectively. At pH 7.0, 8.6, and 11.0, favorable efficacies were attained (57.50, 83.88, and 73.85%, respectively). Additionally, the pH values were found to be altering over the course of various initial pH reactions, presenting a strong buffering capability of the reaction (data not shown).

Acidic condition can boost the dissolution of ZVI into amounts of dissociative ferrous ions, reducing the catalytic activity area. Besides, the presence of excessive $H^+$ would gradually protonate $Fe^{II}$EDTA to form $Fe^{II}$(EDTA H) or $Fe^{II}$(EDTA $H_2$) ligand, whose capability to activate $O_2$ was much lower than its predecessor (Belanzoni et al. 2009; Hong et al. 2009). These could be the explanation for lower removal potency of AAs under acidified US/ZEA system. Most importantly, however, neutral or slightly alkaline circumstances were much preferable for the disposal of sludge and soil, which suggests momentous meaning for practical applications.

## Comparison of AA degradation in different systems

Figure 3 compares the time courses (0–60 min) of AA degradation in residual sludge withdrawn from the US, ZEA, and US/ZEA systems at ambient pH (i.e., 8.6). As can be seen, five AA degradation efficiencies of three processes were US/ZEA (83.88%) > ZEA (72.27%) > US (51.03%) within 60 min and US/ZEA (92.40%) > ZEA (72.88%) > US (51.79%) within 90 min, suggesting US and ZEA have a synergistic effect on AA degradation.

A rapid removal of more than 70% AAs was achieved by ZEA within 30 min, confirming that this process possesses enormous potential in ROS generation. Subsequently, however, a lag period in the ZEA process lasted 90 min, due to the unavailability of contaminants absorbed in the cavities of sludge as well as the inactivity of the inert ZVI surface. While in the US/ZEA, the removal efficiency of AAs increased steadily over time, so did the elimination of SOM contents (Fig. 2a), with a decrease by 51.76% after 120-min reaction. Noteworthy, the degradation rate of EDTA in the US/ZEA system (29.14%) was approximately two-fold higher than the one in the ZEA process (11.82%) after 60-min reaction.

TOC in the filtrate, however, boosted right after ultrasound exposure, leading to a two-fold increase in the TOC content within 40 min. This suggests that the acoustic energy released by US can shred the extracellular polymeric substances in TDS flocs, thus expelling large quantity of organic matters into the soluble phase, and that US was weak in direct mineralization, therefore producing abundant intermediates that would flee to the supernatant (Fig. 2b). As revealed by particle size measurement, sludge particles treated by US were finer,

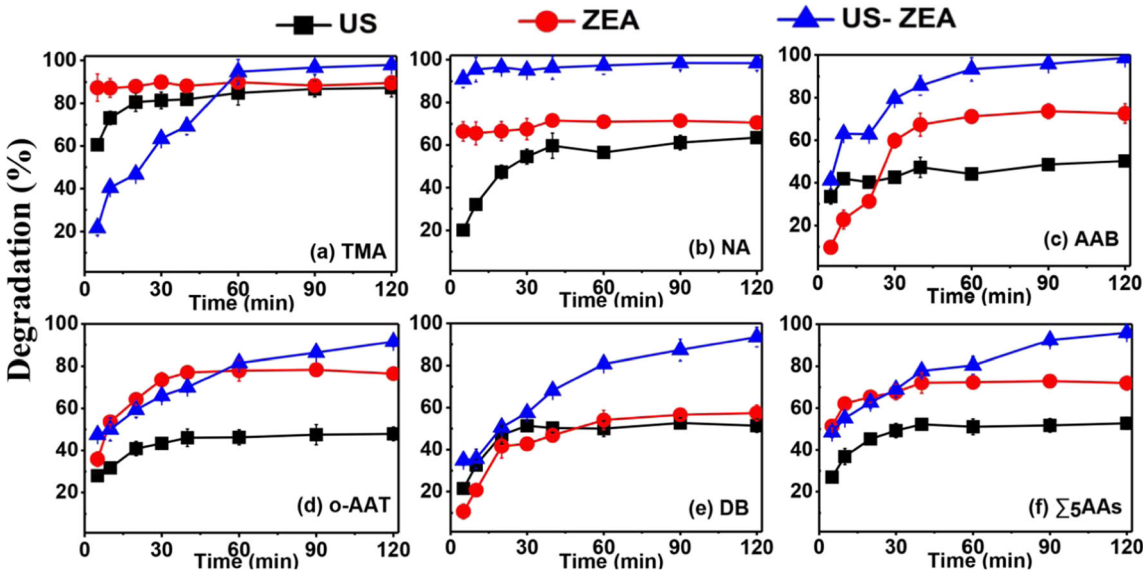


**Fig. 3** Comparison of US, ZEA, and US/ZEA treatments on the removal of different AAs. Initial condition: ZVI = 15 g/L; EDTA = 1.0 mM; ultrasonic power = 1.08 W/cm$^3$ under natural conditions

with $dv_{50}$ decreasing from 145 to 50 μm, confirming ultrasound's ability in tearing incompact macroflocs into smaller fragments. Therefore, conclusively, the promotional role of US mainly lies in sludge disintegration rather than ROS production.

Data showed that the removal efficiencies increased with prolonged time for each AA investigated, and, in the case of the US/ZEA treatment, the degradation efficiencies of TMA, NA, and AAB were noticeably higher than those of o-AAT and DB. Bogan and Trbovic (2003) reported that the majority of hydrophobic organic compounds (HOCs) would sorb onto SOM provided that the solid matrix contains over 5% of organic matter. While organics with lower hydrophobicity would be trapped in the hydrophilic adsorption sites of higher-polarity SOM (Wang et al. 2011), where the formation of ROS would be localized and kept away from HOCs in the microenvironment (Lindsey and Tarr 2000). Therefore, TMA and NA were more easily decomposed than the hydrophobic ones. Besides, US/ZEA displayed low efficiency on TMA, a monocyclic aniline, compared to US and ZEA at the beginning but removed over 96% of TMA in the end. It can be concluded that in the US/ZEA system, complicated molecules would be first decomposed into compounds with smaller molecule weight, and, until then, will further mineralization take place.

As for aromatic amines in the filtrate, only a few TMA, NA, and AAB were detected, suggesting mildly hydrophilic aromatic amines can be transferred to the soluble phase. No o-AAT and DB were determined due to their hydrophobic characteristics, but AAB's content in raw sludge was so massive that few of it released to the filtrate regardless of its hydrophobic property. As can be seen from Fig. S2, TMA in the filtrate showed a rise and fall trend as the same result previously discussed, while NB and AAB gradually decreased with time after being exposed to different treatments. Nevertheless, considering that the contents of these aromatic amines in the supernatant were considerably lower than those in the sludge sample, only contaminants in the solid matrix will be discussed in this paper.

## Role of iron oxides in sludge matrix

TDS is mainly composed of two parts—the coagulating sedimentation of wastewater treated by a coagulant, mainly consisting of $FeSO_4$ and CaO, and the microbial population of anaerobic–aerobic process, in which iron elements exist commonly and diversely. Therefore, considerable sum of Fe can be detected in TDS, which is further confirmed by XPS and XRF tests. XPS testifies that these Fe compositions are existing in the form of various kinds of oxides, i.e., Fe (II)-oxide and Fe(III)-oxide. By XRF analysis, Fe occupied 51.8% of the metal element components in TDS.

Interestingly, Fe content in the US-treated sludge decreased by 4.55% (Fig. 4c), which is consistent with XPS results (Fig. 4a, b, decrease mainly seen in Fe[III]-oxide). The concentration of soluble $Fe^{3+}$, however, was increased by 39.61%, which revealed that the acoustic energy could dissolve sludge iron into soluble ions. Furthermore, $Fe^{3+}$ in the ZEA system maintained at the same level for 60 min, implying that these ions were primarily generated by the dissolution of ZVI and circulated in the iron cycle. While in the US/ZEA system, the drastic raise of $Fe^{3+}$ subsequently decreased and leveled off for the rest 30 min, demonstrating that sludge iron participated in the iron redox cycle of the Fenton-like process, which facilitated subsequent ROS generation.

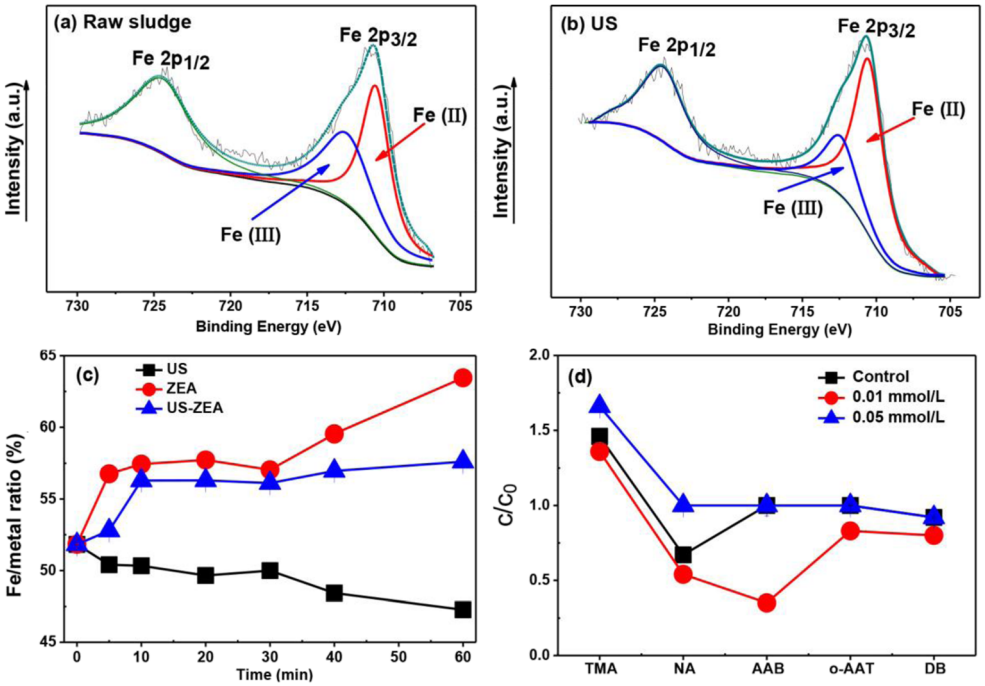


**Fig. 4** XPS Fe 2p spectra for (**a**) raw sludge and (**b**) sludge treated by US; (**c**) XRF-detected Fe oxide (%) in sludge treated by different processes during 0–60 min; (**d**) AA removal in EDTA/air system (air = 1.0 L/min) with different EDTA dosages

It has been found that iron-containing sludge possesses extraordinarily effective catalytic properties on organic removal even in comparison with classical Fenton reagents (Bolobajev et al. 2014) and that chelating agents, like EDTA, could enhance the performance of iron mineral-containing matrix at near neutral circumstances via reductive/non-reductive iron dissolution (Wang et al. 2008). Therefore, for purpose of investigating the latent effect of iron oxides which are largely present in the sludge matrix, experimentation was conducted on sole addition of EDTA and aeration (1.0 L/min). The control group was carried out by aerating 1.0 L/min air into the sludge for 60 min. Figure 4d shows that in the control group, there were 33.58% NA and 8.09% DB removed, while none of AAB or o-AAT was degraded. Noticeably, the concentration of TMA was 1.46 times higher in the control group, which may be due to the decomposition of polycyclic amines (such as NA) into monocyclic ones after aeration. The addition of merely 0.01 mM EDTA surprisingly brought a significant increase in AA removal, with 65.42% of AAB being wiped out. However, when the dosage of EDTA increased to 0.05 mM, the degradation rate of each AA shows little distinction from the control group, which is in common with the discussion that excessive EDTA would exert superior competitiveness upon AAs.

Besides, no soluble ferrous ions were detected and no significant difference was found in the ferric concentration of all groups (Fig. S2). Accordingly, it is deductive that degradation of AAs in the EDTA/air system should be attributed to heterogeneous catalytic reaction over the iron oxides in situ modified by EDTA.

## Main oxidative radicals in US/ZEA system

To verify the predominant oxidants in the US/ZEA system, four different scavengers were utilized to investigate their contributions on each AA degradation. Among the four scavengers, DMSO is a well-known ·OH radical and ferryl ion scavenger is frequently used to evaluate the oxidant generated in Fenton and ZVI systems (Tao et al. 2016; Xie et al. 2009), while TBA was just effective in quenching ·OH ($k_{TBA/OH}$ = 3.8–7.6 × $10^8$ $M^{-1}$ $s^{-1}$). SOD could be used as a scavenger for $O_2^{\cdot-}$, and CAT was chosen as a probe for $H_2O_2$ (Tao et al. 2016).

Figure 5 shows the contribution of different ROS for AA degradation in the US/ZEA system after 60-min reaction. It is observed that the scavengers' sequence in

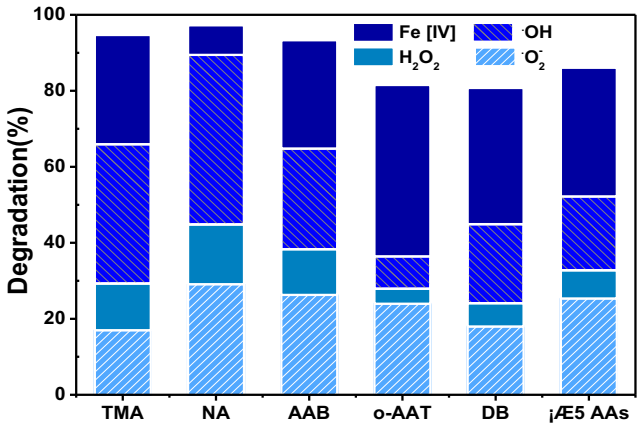


**Fig. 5** The contributions of four oxidant species for AA removal by 60-min US–ZEA treatment

inhibiting AA degradation was DMSO (33.84%) > SOD (25.36%) > TBA (19.44%) > CAT (7.43%), suggesting DMSO highly suppressed AA degradation in the US/ZEA system. It has been reported that ferryl ion was the substitute oxidant for ·OH (Remucal et al. 2011) in the circumneutral or slightly alkaline Fenton/Fenton-like reaction. While SOD and TBA could also decelerate the AA degradation rate to some extent. However, the direct contribution of $H_2O_2$ was relatively unnoticeable, and DPD method failed to detect $H_2O_2$, which implied that the in situ production and its consumption would be considerably rapid. Thereby, the in situ generation of $H_2O_2$ during the series of $Fe^0$–EDTA reactions was more critical in generating most of ·OH by Fenton reaction rather than in direct oxidation of pollutants. Therefore, in the presence of EDTA, another part of ferryl ion ($[Fe^{IV}O]^{2+}$) and ·OH production via Fenton-like reaction were deduced as Eqs. (3)–(4), which was modified by EDTA based on Eq. (3) in the ZVI/air system.

$$Fe^{II}EDTA + H_2O_2 \rightarrow Fe^{III}EDTA + \cdot OH + OH^- \quad (3)$$

$$Fe^{II}EDTA + H_2O_2 \rightarrow \left(Fe^{IV}O\right)^{2+} + H_2O + EDTA \quad (4)$$

### The promotional role of US in the US/ZEA system

According to the discussion mentioned previously, the ZEA reaction scheme (Fig. S4) in TDS was proposed with or without the promotional role of US.

In the ZEA system, EDTA would first complex with $Fe^{2+}$ on the thin pristine $Fe_xO_y$ layer of ZVI by initiating the so-called "point dissolution" (Xiang et al. 2016), which generates $Fe^{II}EDTA$ and $Fe^{III}EDTA$. A redox reaction cycle between the two ligands based on ZVI would be formed on the disposed $Fe^0$(s) surface, and, then, homogeneous oxygen activation would be realized. Herein, abundant ROS (the "Main oxidative radicals in US/ZEA system" section), including ·OH, $O_2^{\cdot -}$, and Fe(IV), would come into being and oxidize AAs adsorbing onto the sludge surface as well as SOM. Due to the promising chelating coefficients with ferrous and ferric ions, at the beginning, the release of $Fe^{2+}$ species on the ZVI surface would be accelerated by enough EDTA. As time prolonged, however, EDTA was degraded into low-molecular acids and the surface layer would be covered by thick iron oxides resulting from the corrosion of $O_2$ and protons (see Fig. 6b), which retards the production of in situ $H_2O_2$ and the subsequent ROS. Thereafter, the degradation efficiency of AAs is limited (the "Comparison of AA degradation in different systems" section).

As for the facilitating role of US, it can be comparatively complicated, mainly functioning in chemical and physical effects. Physically, on the one side, US would disintegrate sludge into finer particles, in the cavities of which AAs would be uncovered and exposed to the liquid phase (see Fig. S2); on the other side, enhanced stripping and dissolution of iron oxide layer was realized by cavitation effects, thus maintaining the reactivity of ZVI surface and enhancing solid–liquid interfacial mass transfer (Cai et al. 2016). This was confirmed by SEM (Fig. 6). Noticeably, the pristine ZVI showed a considerably smooth surface (Fig. 6a), while for ZEA-treated ZVI, a denser coverage of oxide precipitates was formed on the surface due to the aeration (Fig. 6b). However, the introduction of ultrasound destroyed the thick coverings and promoted in-depth corrosion of the inside pristine ZVI (Fig. 6c), as a result of which, the surface layer of ZVI became lumpy and devastated in the US/ZEA system. Besides, the acoustic streaming would also enhance dispersion of iron particles and free radical transfer toward the slurry. Sono-chemically, the acoustic cavitation releases hydroxyl radicals according to our previous study (Ning et al. 2014). Besides, it would also dissolve the sludge iron oxides into soluble ions which directly participate in the iron cycle to promote the ROS generation (the "Role of iron oxides in sludge matrix" section). Therefore, the combination of US and ZEA could facilitate the efficiency of AA degradation in TDS.

## Conclusion

This study indicated that US/ZEA can lead to effective removal of AAs from textile dyeing sludge. In situ generation of ROS was achieved by $O_2$ activation based on the solid–liquid interfacial reaction between ZVI and EDTA under neutral or slightly alkaline circumstances, wherein significant synergy was manifested by the enhancement of removal and the shortening of the lag period by ZEA alone. Several principal parameters were verified to be critical for AA degradation, and the initial condition was optimized as 1.08 W/cm$^3$ ultrasound power, 15 g/L ZVI, 1.0 mM EDTA, and original pH 8.60 to achieve 92.40% removal with 90-min reaction time. Moreover, iron oxides in the sludge can also establish a heterogeneous catalytic system with EDTA to degrade AAs. The reaction mechanism with the promotion of US was proposed for the system, where three ROS (Fe[IV], $O_2^{\cdot -}$, and ·OH) instead of ·OH alone would dominate the oxidation. US plays a major role in disintegrating the sludge particles and releasing SOM, thoroughly exposing contaminants to ROS;

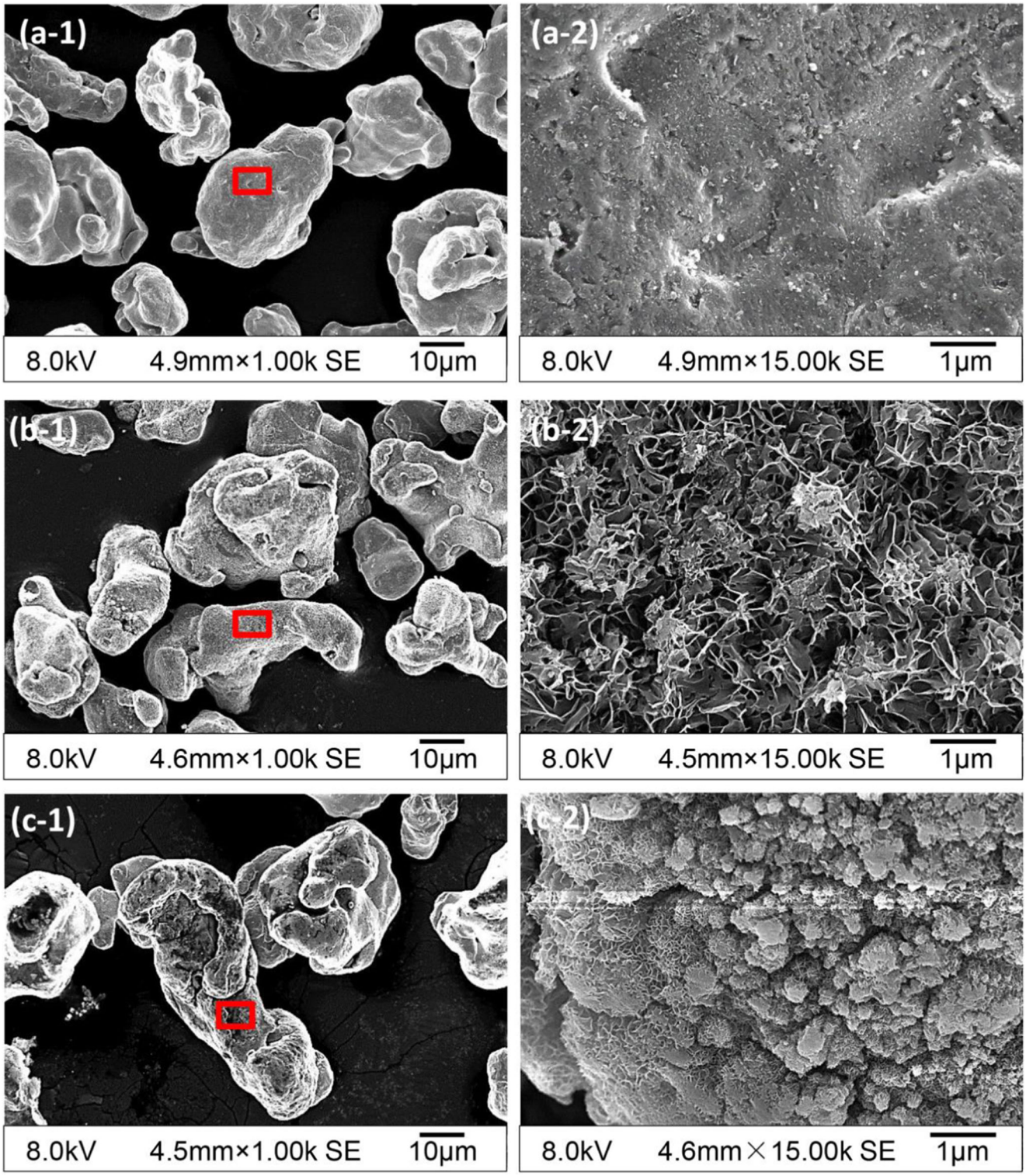


**Fig. 6** SEM images of (**a**) original ZVI, (**b**) ZVI after 60-min ZEA reaction, and (**c**) ZVI after 60-min US/ZEA reaction

meanwhile, it alters and facilitates the heterogeneous surface corrosion of ZVI, which triggers no change to the homogeneous iron cycle as well as the Fenton reactions. Still, a further insight into the detoxification effects of the integrated technique on textile dyeing sludge is expected.

**Acknowledgements** This study is financially supported by the Science and Technology Plan of Guangzhou (No. 201607010330), the Science and Technology Plan of Guangdong Province (No. 2015A020215032), the Special Applied Technology Research and Development of Guangdong Province (major project) (No. 2015B020235013), and the Natural Science Foundation of China (No. 21577027).

## References


And CEN, Cheng IF (2005) EDTA degradation induced by oxygen activation in a zerovalent iron/air/water system. Environ Sci Technol 39: 7158–7163

Bagal MV, Gogate PR (2012) Sonochemical degradation of alachlor in the presence of process intensifying additives. Sep Purif Technol 90:92–100

Bagal MV, Gogate PR (2014) Wastewater treatment using hybrid treatment schemes based on cavitation and Fenton chemistry: a review. Ultrason Sonochem 21:1–14

Belanzoni P, Bernasconi L, Baerends EJ (2009) $O_2$ activation in a dinuclear Fe(II)/EDTA complex: spin surface crossing as a route to highly reactive Fe(IV)oxo species. J Phys Chem A 113:11926–11937

Bogan BW, Trbovic V (2003) Effect of sequestration on PAH degradability with Fenton's reagent: roles of total organic carbon, humin, and soil porosity. J Hazard Mater 100:285–300

Bolobajev J, Kattel E, Viisimaa M, Goi A, Trapido M, Tenno T, Dulova N (2014) Reuse of ferric sludge as an iron source for the Fenton-based process in wastewater treatment. Chem Eng J 255:8–13

Cai M, Su J, Lian G, Wei X, Dong C, Zhang H, Jin M, Wei Z (2016) Sono-advanced Fenton decolorization of azo dye Orange G: analysis of synergistic effect and mechanisms. Ultrason Sonochem 31:193–200

Deng M, Kuo D, Wu Q, Zhang Y, Liu X, Liu S, Hu X, Mai B, Liu Z, Zhang H (2018) Organophosphorus flame retardants and heavy metals in municipal landfill leachate treatment system in Guangzhou, China. Environ Pollut 236:137–145

Ghods P, Isgor OB, Brown JR, Bensebaa F, Kingston D (2011) XPS depth profiling study on the passive oxide film of carbon steel in saturated calcium hydroxide solution and the effect of chloride on the film properties. Appl Surf Sci 257:4669–4677

Hong S, Lee YM, Shin W, Fukuzumi S, Nam W (2009) Dioxygen activation by mononuclear nonheme iron(II) complexes generates iron–oxygen intermediates in the presence of an NADH analogue and proton. J Am Chem Soc 131:13910–13911

Huang M, Tao Z, Wu X, Mao J (2017) Distinguishing homogeneous-heterogeneous degradation of norfloxacin in a photochemical Fenton-like system ($Fe_3O_4$/UV/oxalate) and the interfacial reaction mechanism. Water Res 119:47–56

Huang YH, Zhang TC (2005) Effects of dissolved oxygen on formation of corrosion products and concomitant oxygen and nitrate reduction in zero-valent iron systems with or without aqueous $Fe^{2+}$. Water Res 39:1751–1760

Englehardt JD, Meeroff DE, Echegoyen L, Deng Y, Raymo a FM, Shibata T (2007) Oxidation of aqueous EDTA and associated organics and coprecipitation of inorganics by ambient iron-mediated aeration. Environ Sci Technol 41:270–276

Joshi SM, Gogate PR (2019) Treatment of landfill leachate using different configurations of ultrasonic reactors combined with advanced oxidation processes. Sep Purif Technol 211:10–18

Jr AEH, Smart JA, Amis ES (1955) Simultaneous spectrophotometric determination of iron(II) and total iron with 1,10-phenanthroline. Anal Chem 27:26–29

Lee B-D, Iso M, Hosomi M (2001) Prediction of Fenton oxidation positions in polycyclic aromatic hydrocarbons by frontier electron density. Chemosphere 42:431–435

Lee H, Lee HJ, Kim HE, Kweon J, Lee BD, Lee C (2014) Oxidant production from corrosion of nano- and microparticulate zero-valent iron in the presence of oxygen: a comparative study. J Hazard Mater 265:201–207

Li H, Jin Y, Mahar RB, Wang Z, Nie Y (2009) Effects of ultrasonic disintegration on sludge microbial activity and dewaterability. J Hazard Mater 161:1421

Li H, Wan J, Ma Y, Huang M, Yan W, Chen Y (2014) New insights into the role of zero-valent iron surface oxidation layers in persulfate oxidation of dibutyl phthalate solutions. Chem Eng J 250:137–147

Lin M, Ning XA, An T, Zhang J, Chen C, Ke Y, Wang Y, Zhang Y, Sun J, Liu J (2016) Degradation of polycyclic aromatic hydrocarbons (PAHs) in textile dyeing sludge with ultrasound and Fenton processes: effect of system parameters and synergistic effect study. J Hazard Mater 307:7–16

Lindsey ME, Tarr MA (2000) Inhibited hydroxyl radical degradation of aromatic hydrocarbons in the presence of dissolved fulvic acid. Water Res 34:2385–2389

Meng XZ, Venkatesan AK, Ni YL, Steele JC, Wu LL, Bignert A, Bergman Å, Halden RU (2016) Organic contaminants in Chinese sewage sludge: a meta-analysis of the literature of the past 30 years. Environ Sci Technol 50:5454–5466

Mhetre AS, Gogate PR (2014) New design and mapping of sonochemical reactor operating at capacity of 72L. Chem Eng J 258:69–76

Ning X-a, Chen H, Wu J, Wang Y, Liu J, Lin M (2014) Effects of ultrasound assisted Fenton treatment on textile dyeing sludge structure and dewaterability. Chem Eng J 242:102–108

Ning XA, Liang JY, Li RJ, Hong Z, Wang YJ, Chang KL, Zhang YP, Yang ZY (2015) Aromatic amine contents, component distributions and risk assessment in sludge from 10 textile-dyeing plants. Chemosphere 134:367–373

Patil AL, Patil PN, Gogate PR (2014) Degradation of imidacloprid containing wastewaters using ultrasound based treatment strategies. Ultrason Sonochem 21:1778–1786

Remucal CK, Lee C, Sedlak DL (2011) Comment on "oxidation of sulfoxides and arsenic(III) in corrosion of nanoscale zero valent iron by oxygen: evidence against ferryl ions (Fe(IV)) as active intermediates in Fenton reaction". Environ Sci Technol 45:3177–3178

Segura Y, Martínez F, Melero JA, Fierro JLG (2015) Zero valent iron (ZVI) mediated Fenton degradation of industrial wastewater: treatment performance and characterization of final composites. Chem Eng J 269:298–305

Sivasankar T, Moholkar VS (2009) Physical insights into the sonochemical degradation of recalcitrant organic pollutants with cavitation bubble dynamics. Ultrason Sonochem 16:769–781

Sommaggio LRD, Pamplona-Silva MT, Marin-Morales MA (2018) Evaluation of the potential agricultural use of biostimulated sewage sludge using mammalian cell culture assays. Chemosphere 199:10–15

Stefaniuk M, Tsang D, Ok YS, Oleszczuk P (2018) A field study of bioavailable polycyclic aromatic hydrocarbons (PAHs) in sewage sludge and biochar amended soils. J Hazard Mater 349:27–34

Tao Z, Zou X, Mao J, Wu X (2016) Decomposition of sulfadiazine in a sonochemical Fe0-catalyzed persulfate system: parameters optimizing and interferences of wastewater matrix. Appl Catal B Environ 185:31–41

Wang X, Liu C, Li X, Li F, Zhou S (2008) Photodegradation of 2-mercaptobenzothiazole in the gamma-Fe(2)O(3)/oxalate suspension under UVA light irradiation. J Hazard Mater 153:426–433

Wang X, Guo X, Yang Y, Tao S, Xing B (2011) Sorption mechanisms of phenanthrene, lindane, and atrazine with various humic acid fractions from a single soil sample. Environ Sci Technol 45:2124–2130

Xiang W, Zhang B, Zhou T, Wu X, Mao J (2016) An insight in magnetic field enhanced zero-valent iron/$H_2O_2$ Fenton-like systems: critical role and evolution of the pristine iron oxides layer. Sci Rep 6:24094

Xie F, Cai T, Ma Y, Li H, Li C, Huang Z, Yuan G (2009) Recovery of Cu and Fe from printed circuit board waste sludge by ultrasound: evaluation of industrial application. J Clean Prod 17:1494–1498

Zhang J, Li J, Thring R, Liu L (2013) Application of ultrasound and Fenton's reaction process for the treatment of oily sludge. Procedia Environ Sci 18:686–693

Zhou H, Qian S, Xun W, Wang L, Jing C, Zhang J, Lu X (2014) Removal of 2,4-dichlorophenol from contaminated soil by a heterogeneous ZVI/EDTA/air Fenton-like system. Sep Purif Technol 132:346–353

Zhou T, Lim TT, Li Y, Lu X, Wong FS (2010) The role and fate of EDTA in ultrasound-enhanced zero-valent iron/air system. Chemosphere 78:576–582